Proton MR spectroscopy in acute middle cerebral artery stroke.

J H Gillard, P B Barker, P C van Zijl, R N Bryan and S M Oppenheimer

AJNR Am J Neuroradiol 1996, 17 (5) 873-886
http://www.ajnr.org/content/17/5/873

Proton MR Spectroscopy in Acute Middle Cerebral Artery Stroke

Jonathan H. Gillard, Peter B. Barker, Peter C. M. van Zijl, R. Nick Bryan, and Stephen M. Oppenheimer

PURPOSE: To investigate the feasibility of performing multisection proton MR spectroscopy in patients with acute stroke, and to determine whether this imaging technique can depict ischemic or infarcted brain regions. **METHODS:** Multisection proton MR spectroscopy, MR imaging, and MR angiography were performed within 24 hours of stroke onset (mean, 12 hours) in 12 patients who had had a stroke of the middle cerebral artery. Spectra were analyzed from brain regions containing T2 hyperintensity abnormalities on MR images, from regions immediately adjacent to these abnormalities, and from anatomically similar contralateral regions. Areas of brain containing lactate were compared with areas of T2 hyperintensities on MR images. **RESULTS:** One data set was discarded because of excessive artifacts from patient motion. Regions of T2 hyperintensities on MR images were found to contain elevated lactate (all 11 cases) and reduced *N*-acetyl-aspartate (10 of 11 cases) relative to contralateral measurements. Lactate levels in regions adjacent to T2 hyperintensities were not significantly different from those of infarcted brain. On the other hand, *N*-acetyl-aspartate was significantly lower in regions of infarction compared with periinfarct tissue. Areas of brain containing elevated lactate significantly exceeded those of T2 abnormality. **CONCLUSIONS:** Proton MR spectroscopy is feasible for imaging patients with acute stroke. In the early stages of stroke, tissue containing elevated lactate but no other spectroscopic or MR imaging abnormality can be identified. Such regions may represent an ischemic zone at risk of infarction.

Index terms: Arteries, cerebral, middle; Brain, infarction; Magnetic resonance, spectroscopy

AJNR Am J Neuroradiol 17:873–886, May 1996

Findings on conventional magnetic resonance (MR) images are generally either normal or nonspecific during the early stages of ischemia, and do not provide information concerning areas at risk of infarction (1, 2). Proton MR spectroscopy, however, is able to provide information about metabolic changes that may occur before the onset of changes seen on computed tomographic (CT) scans or T2-weighted MR images in the acute setting (3). Various metabolite signals may be detected in a proton MR spectrum, including lactate, an indicator of ischemia in the acute phase of stroke, and *N*-acetyl-aspartate (NAA), believed to be a neuronal marker (4). Proton MR spectroscopy, therefore, in conjunction with MR imaging and MR angiography, has the potential to become a useful diagnostic tool for use in the evaluation of acute stroke.

The earliest studies of proton MR spectroscopy in human stroke used single-voxel localization techniques (5, 6). With the use of this methodology, it has been found that elevated lactate and decreased NAA levels can be detected in cases of acute ($<$ 24 hours) (7–10), subacute (24 hours to 7 days) (6, 10, 11), and late subacute ($>$ 7 days) (5, 7, 11–14) stroke. Single-voxel techniques, however, do not provide information regarding the spatial distribution and extent of metabolic abnormalities, and require that the location of the ischemic or infarcted region be already known or visible on MR images. There have, therefore, been efforts to develop spectroscopic imaging methods for the study of cerebral ischemia, either in one (15–17) or two (18–20) spatial dimensions. A single case study of a patient with acute stroke

Received July 18, 1995; accepted after revision November 17.

Supported by the Whitaker Foundation, Washington, DC, and National Institutes of Health grant 3R01NS31490.

From the Departments of Radiology (J.H.G., P.B.B., P.C.M.vZ., R.N.B.) and Neurology (J.H.G., S.M.O.), The Johns Hopkins Medical Institutions, Baltimore, Md.

Address reprint requests to Peter B. Barker, DPhil, Department of Neurology, Henry Ford Hospital, 2799 W Grand Blvd, Detroit, MI 48202.

AJNR 17:873–886, May 1996 0195-6108/96/1705–0873

has been reported (3) in which researchers used the newly developed technique of multisection spectroscopic imaging (21). The purpose of this investigation was to use multisection proton MR spectroscopy to study 12 patients in whom acute stroke of the middle cerebral artery (MCA) had been diagnosed.

Subjects and Methods

Five men and seven women with acute stroke of the MCA were studied. Their mean age was 62 ± 13 years; three had a history of stroke and 2 had a history of transient ischemic attacks; three were diabetic and nine had a history of hypertension. The mean time from onset of stroke to MR spectroscopy was 12 hours (range, 2 to 24 hours). In addition, an asymptomatic 74-year-old male volunteer was studied as a control subject.

MR studies were done on a 1.5-T scanner. The scanning protocol consisted of six series, with a total scan time of approximately 90 minutes. In the first two series, sagittal T1 localizer images were obtained followed by axial double-echo T2-weighted images. The third and fourth series consisted of time-of-flight MR angiography of the carotid artery bifurcation (series 3) and intracranial vessels (series 4) in the region of the circle of Willis. For series 5, a set of four oblique axial T1-weighted spin-echo MR images (400/20/1 [repetition time/echo time/excitations]) was obtained at the same section locations and thicknesses as for the MR spectroscopic sections in series 6 (see following description) for anatomic coregistration of the metabolic images and prescription of outer-volume saturation section locations. Series 6 involved multisection two-dimensional proton MR spectroscopy with a spin-echo pulse sequence with octagonal outer-volume saturation pulses and water suppression using a chemical-shift selective saturation sequence (21–23). Four 15-mm-thick oblique sections (2300/272/1) were interleaved with a gap of 2.5 mm. Field homogeneity was optimized manually (5 minutes) by means of linear (X, Y, and Z) shim corrections only over the entire volume covered by the four MR spectroscopic sections. The size of the MR spectroscopic data matrix was 32 × 32 × 256 points; a circular k-space sampling scheme resulted in a total data acquisition time of 30 minutes. The nominal in-plane resolution was 7.5 × 7.5 mm, leading to a nominal voxel size of approximately 0.8 cm^3. MR spectroscopic data sets were processed with multidimensional Fourier transformation after cosine apodization in the k-space domains, and exponential filtering in the time-domain corresponding to a line broadening of 3 Hz. Residual water signals were removed by digital high-pass filtration (24). A susceptibility correction was applied to each voxel's spectra and was based on the frequency of the NAA peak; the program searched for the NAA frequency in each voxel, and then shifted the data left or right so that the NAA peak resonated at exactly 2.02 ppm. Metabolic images were reconstructed from the peaks at 3.2, 3.0, 2.0, and 1.3 ppm, representing choline, creatine, NAA, and lactate, respectively, by integrating peak areas, and linear interpolation by a factor of 8, giving a final image matrix size of 256 × 256. Metabolite images were overlaid with edge-detected MR images (series 5) for anatomic registration.

Sequences 1 through 4 were repeated at 72 hours, or later, after the onset of stroke in 11 of the 12 patients. MR imaging studies were initially interpreted by the attending radiologist (and by one of the authors) on the day of the study with no knowledge of the MR spectroscopic data. In addition, long-repetition-time images were interpreted during analysis of the MR spectroscopic spectra. MR spectroscopic studies were analyzed independently and a consensus was reached. The relative quality of the studies in terms of spectral resolution, lipid contamination, and motion artifacts, when compared with the quality of MR spectroscopic studies obtainable with this technique in healthy volunteers (21), were rated on an arbitrary 4-point scale (1 = poor, 2 = adequate, 3 = good, and 4 = excellent).

Spectroscopic data were analyzed in three ways; first, a region-of-interest approach was used; integrals for choline, creatine, NAA, and lactate were calculated from regions of interest presumed to be infarcted on the basis of MR T2 hyperintensities and from adjacent regions (more than one pixel distant) with a normal T2 MR appearance. These were then compared with spectra from normal-appearing contralateral brain regions in similar anatomic locations. Ratios of ipsilateral to contralateral metabolite integrals were calculated. Since lactate is not detectable in normal brain with the method used in the current study (21), stroke lactate integrals were expressed relative to the contralateral creatine integral (14, 25). Spectra consistent with tissue at risk of infarction were identified if they contained lactate, had a normal MR appearance on T2-weighted sequences, and had a significant NAA content (≥50% compared with the contralateral spectrum). A resonance was only assigned to lactate if it had a chemical shift of exactly 1.33 ppm and a doublet structure with a 7-Hz coupling constant.

In the second part of the spectroscopic analysis, designed to quantify and compare the spatial extent of spectroscopic and MR abnormalities, areas of elevated lactate signal and T2 hyperintensities (in the section exhibiting the greatest abnormalities) were calculated. One of the investigators manually traced the edges of the regions of abnormal signal intensity by using the program Image 1.49 (National Institutes of Health, Bethesda, Md). The program then calculated the area of the manually selected regions. All area measurements were expressed as a function of the total area of the affected hemisphere, including the ventricular spaces. Finally, spectroscopic images were also evaluated visually by two of the investigators to screen for metabolic abnormalities that may not have been detected with either of the above approaches.

A completed MCA stroke was defined as persistence of a neurologic deficit for more than 24 hours and the presence of clinically appropriate T2-weighted MR corroboration of stroke on day 1 and/or day 3 (or later). Statistical

analysis was performed with the nonparametric Wilcoxon's signed rank test using the program Statview II (Abacus Concepts, Berkeley, Calif). Significance was defined as $P = .05$. Ethical approval was obtained from the Joint Committee for Clinical Investigation of the Johns Hopkins Hospital. Informed consent was obtained before patients were included in the study, either directly from the patient or from a close relative.

Results

MR spectroscopy was performed successfully in 11 (92%) of 12 patients; the data set for one patient was discarded owing to motion artifacts. All 4 sections were imaged in 7 (64%) of the 11 patients in whom sets of data were analyzed; only 1 section was imaged in the other 4 patients (36%), because of patient movement or inability to tolerate MR spectroscopy in addition to the T2-weighted and angiographic sequences. No studies were rated as excellent (Table 1).

The mean area of brain regions containing elevated lactate signals was 15% (range, 1% to 96%), expressed as a function of the total ipsilateral hemispheric area. The mean area of T2 abnormality was 5% (range, 0% to 9%). The

TABLE 1: MR spectroscopic findings in 11 patients

Patient	Time of MR Spectroscopy from Stroke Onset, hours	Ratio of Areas of Elevated Lactate to Area of T2 Abnormality	Detection of Tissue at Risk of Infarction	No. of MR Spectroscopic Sections	Quality of MR Spectroscopic Study	Time to Follow-up Study	Progression to Infarction of Tissue at Risk
1	9	1.12	No	4	Good	. . .	. . .
2	21	∞*	Yes	4	Good	Patient died on day 3	. . .
3	7	1.77	Yes	4	Adequate	Day 3	Yes
4	24	2.36	Yes	4	Good	Day 8	Yes†
5	19	1.10	No	1	Poor	. . .	. . .
7	19	3.43	Yes	1	Poor	Day 3	No
8	21	0.15	No	1	Adequate	. . .	. . .
9	2	1.47	Yes	4	Adequate	Day 3	Yes
10	7	1.17	No	4	Adequate	. . .	. . .
11	8	1.84	Yes	1	Good	Day 3	Yes
12	9	0.97	No	4	Poor	. . .	. . .

Note.—Data from patient 6 were discarded owing to excessive artifacts caused by patient motion.

* No T2 hyperintensity was detected.

† Only part of the tissue at risk of infarction (identified on day 1) progressed to infarction on follow-up.

TABLE 2: Metabolite levels in areas of T2 hyperintensity and surrounding areas

Patient	Lactate*		*N*-Actyl Aspartate†		Choline†		Creatine†	
	Area of T2 Abnormality	Region Around Abnormality	Area of T2 Abnormality	Region Around Abnormality	Area of T2 Abnormality	Region Around Abnormality	Area of T2 Abnormality	Region Around Abnormality
1	2.21	. . .	0.53	. . .	1.18	. . .	1.25	. . .
2	4.60	2.71	0.34	0.51	1.18	1.12	1.28	1.27
3	0.65	1.03	0.72	1.09	0.89	1.55	1.14	1.11
4	1.69	1.06	0.70	0.95	1.02	1.22	1.39	1.43
5	5.48	. . .	1.07	. . .	0.70	. . .	1.63	. . .
7	1.99	2.41	0.29	0.66	0.49	1.75	0.49	0.66
8	1.60	. . .	0.47	. . .	0.65	. . .	0.72	. . .
9	1.47	1.05	0.83	1.49	1.28	0.57	0.96	1.36
10	2.24	. . .	0.90	. . .	1.40	. . .	0.93	. . .
11	3.22	3.51	0.56	0.57	0.80	0.69	1.51	1.37
12	0.72	. . .	0.86	. . .	0.70	. . .	0.98	. . .

Note.—Data from patient 6 were discarded owing to excessive artifacts caused by patient motion.

* Lactate integral was expressed as a ratio of the contralateral creatine integral, because no contralateral lactate signals were detectable.

† *N*-acetyl-aspartate, choline, and creatine integrals were expressed as ratios of the integral of the same metabolite in the contralateral voxel.

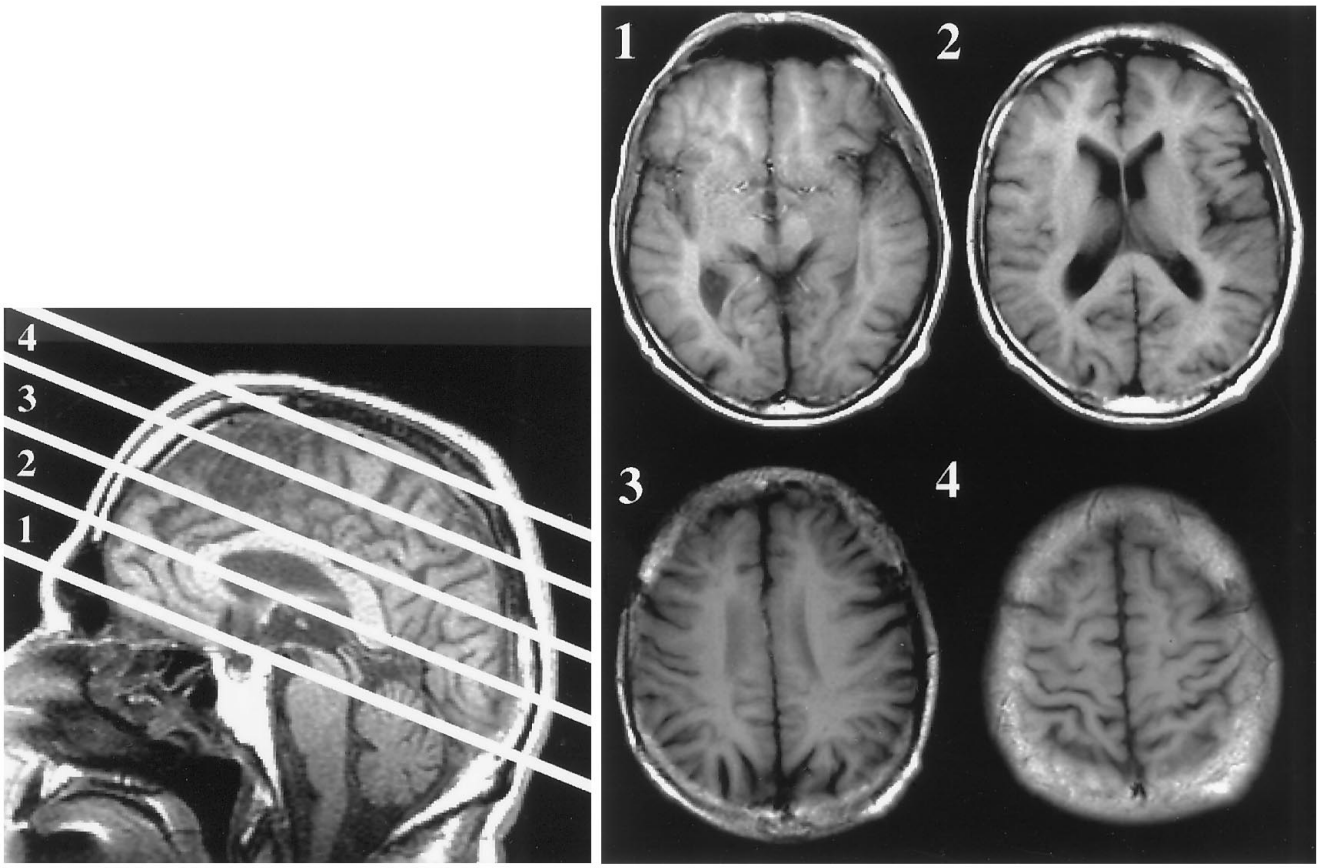

Fig 1. A 74-year-old healthy volunteer.

A, T1-weighted MR images show locations of the four oblique sections used for spectroscopic imaging oriented parallel to the line of the anterior commissure–posterior commissure. *Figure continues.*

ratios of the areas of elevated lactate signal to T2 abnormalities are shown in Table 1. The area of elevated lactate significantly exceeded that of the T2 abnormalities in 9 (82%) of 11 cases ($P = .04$).

Lactate was detected in 11 (100%) of 11 patients who were imaged successfully (Table 2) ($P < .01$ for the area of T2 abnormality and $P < .05$ for the region around the T2 abnormality). NAA was reduced in the areas of T2 abnormality in 10 (91%) of 11 cases as compared with the NAA signal in similarly positioned contralateral areas of interest ($P < .01$). In regions adjacent to the T2 hyperintensities, NAA was not significantly different from contralateral NAA levels ($P = .25$), but was significantly higher than in the area of T2 abnormality ($P < .05$). Choline was not significantly different in either the area of T2 abnormality ($P = .86$) or the adjacent areas ($P = .46$) as compared with the contralateral choline signal.

Figure 1 shows representative spectroscopic images from a 74-year-old volunteer subject. Figure 1A shows the locations of the four 15-mm-thick MR spectroscopic sections. Metabolic images and selected spectra from section 2 are shown in Figure 1B and C. Representative examples of MR spectroscopy and MR imaging from three patients are shown in Figures 2 through 4. Figure 2A is an MR spectroscopic image of patient 2 (with an occluded left internal carotid artery [ICA] and MCA); the figure shows a marked reduction of NAA levels and widespread elevation of lactate in most of the left hemisphere. A relative increase in choline is also seen, particularly in the posterior white matter regions. Representative spectra from each hemisphere are shown in Figure 2B; note the medial region (spectrum 4), which contains both NAA and lactate. T2-weighted MR images showed mild hyperintensity and swelling of the

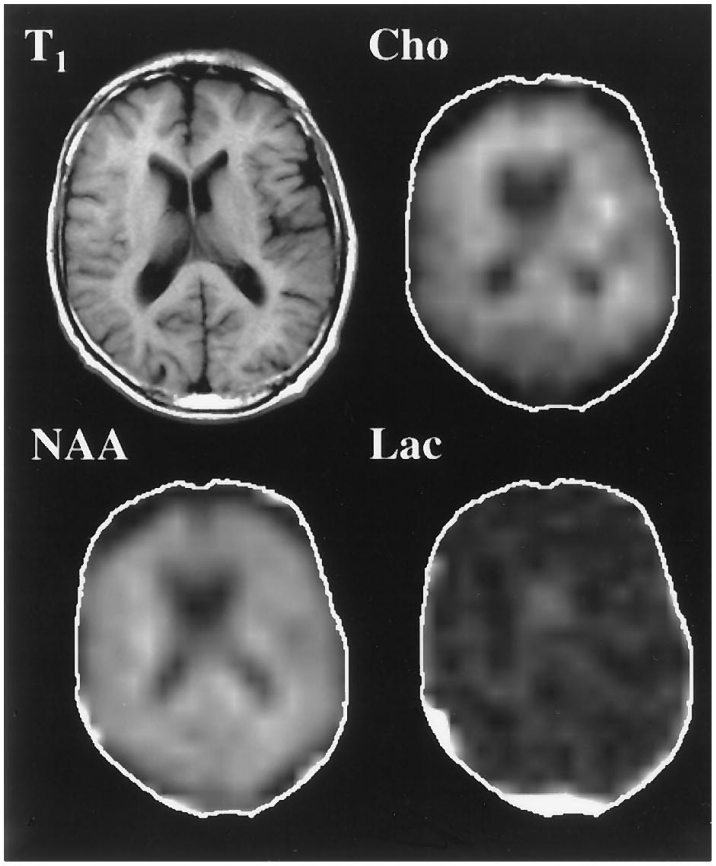

B

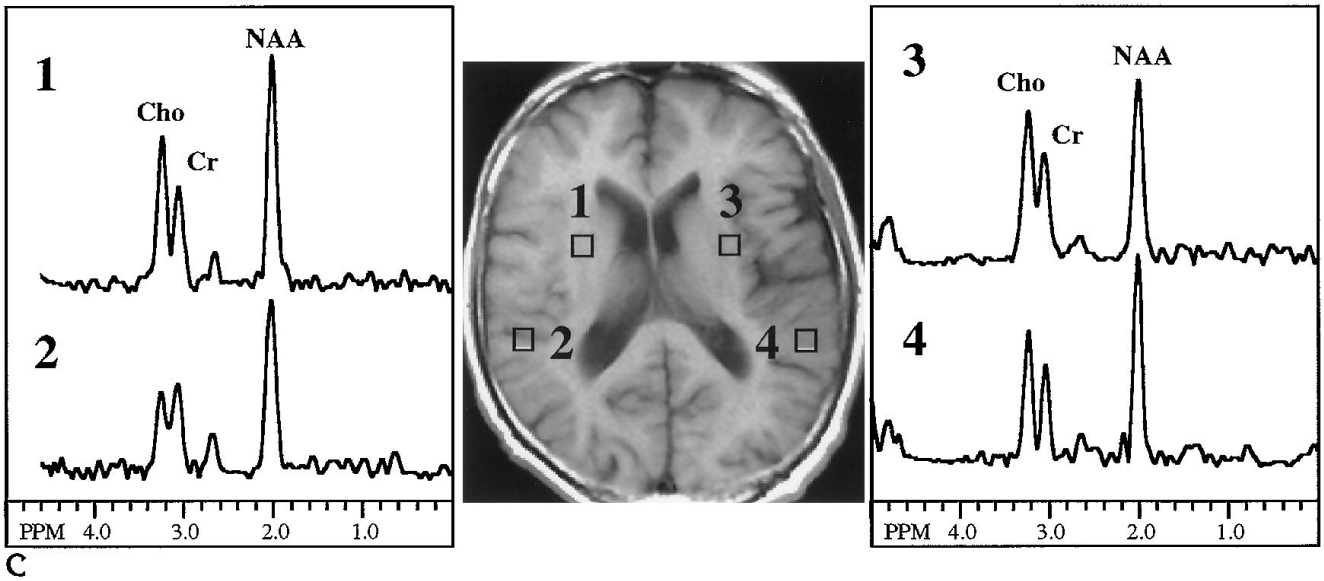

C

Fig 1, *continued.*
B, T1-weighted and spectroscopic images (choline [*Cho*], *N*-acetyl-aspartate [*NAA*], and lactate [*Lac*]) from section 2.
C, Representative spectra from selected voxels of section 2.

Fig 2. Patient 2: tandem occlusion of left internal and middle cerebral arteries was seen at MR angiography.

A, T2-weighted MR image, showing motion artifact, and MR spectrographic images of *N*-acetyl-aspartate (*NAA*), choline (*Cho*), and lactate (*Lac*) from section 2, showing elevated lactate and reduced NAA in the left middle cerebral artery (MCA) and left posterior cerebral artery (PCA) territories. Also note increased choline, particularly in the posterior white matter region (*arrow*).

B, T1-weighted MR image and selected proton spectra show decreased NAA and increased lactate in the infarcted left MCA and PCA territories, essentially normal contralateral metabolism, and a medial region consistent with tissue potentially at risk of infarction with both lactate and preserved NAA (voxel 4).

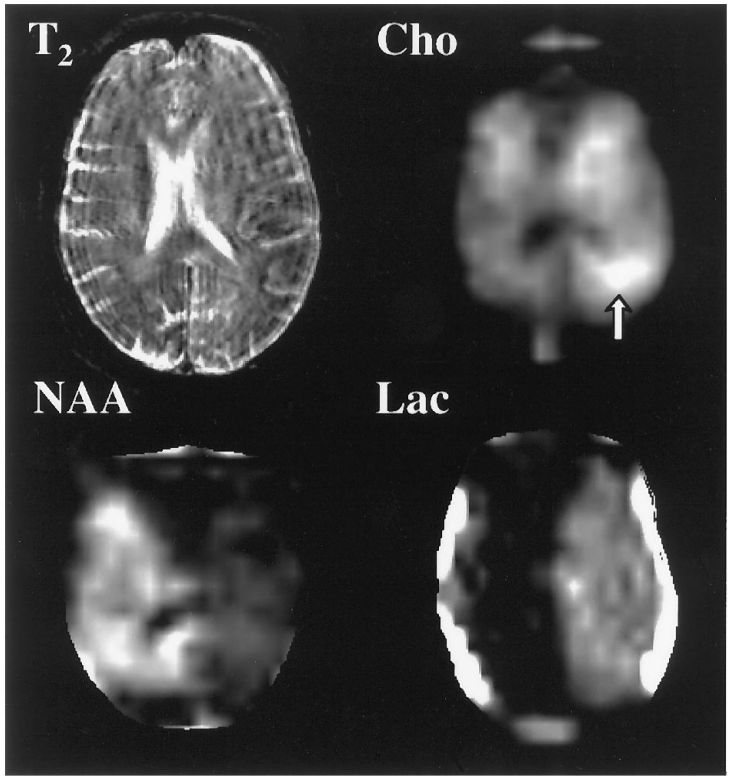

A

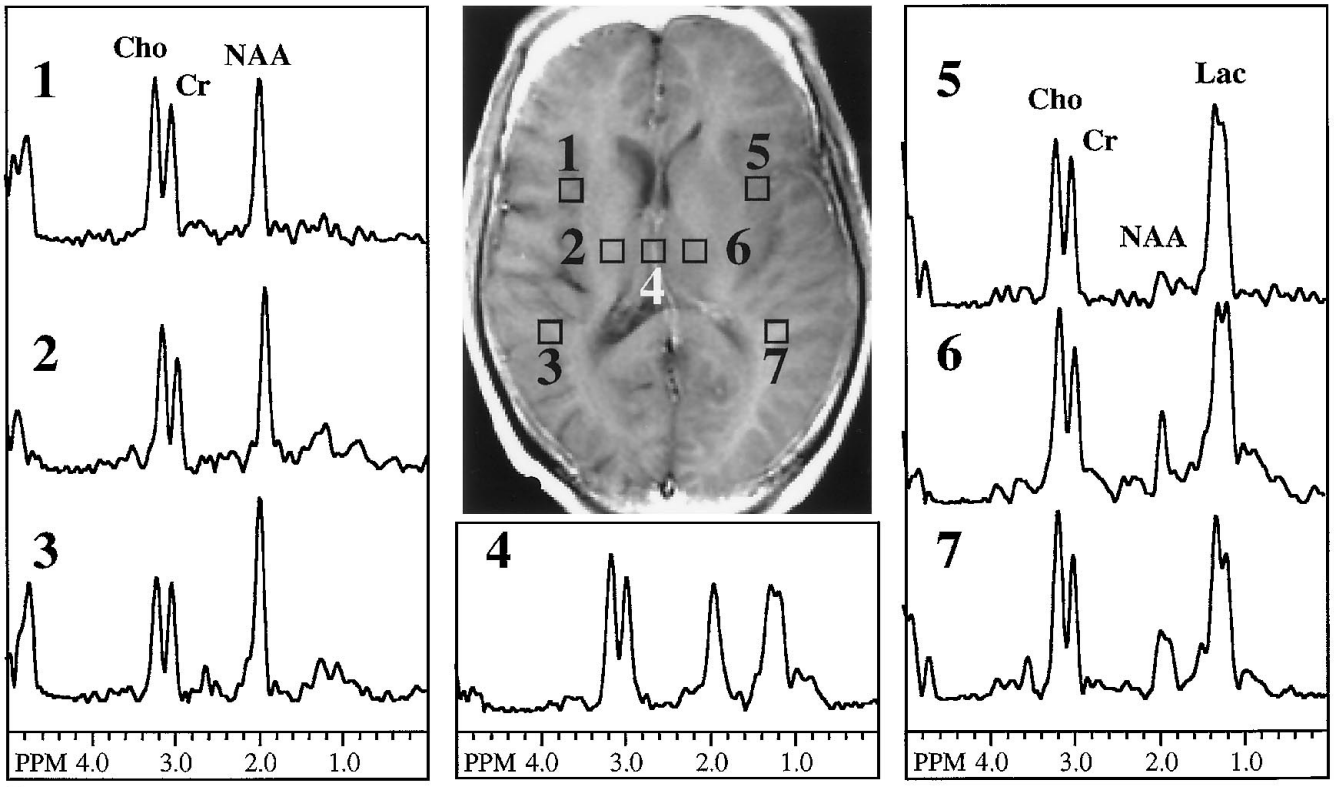

B

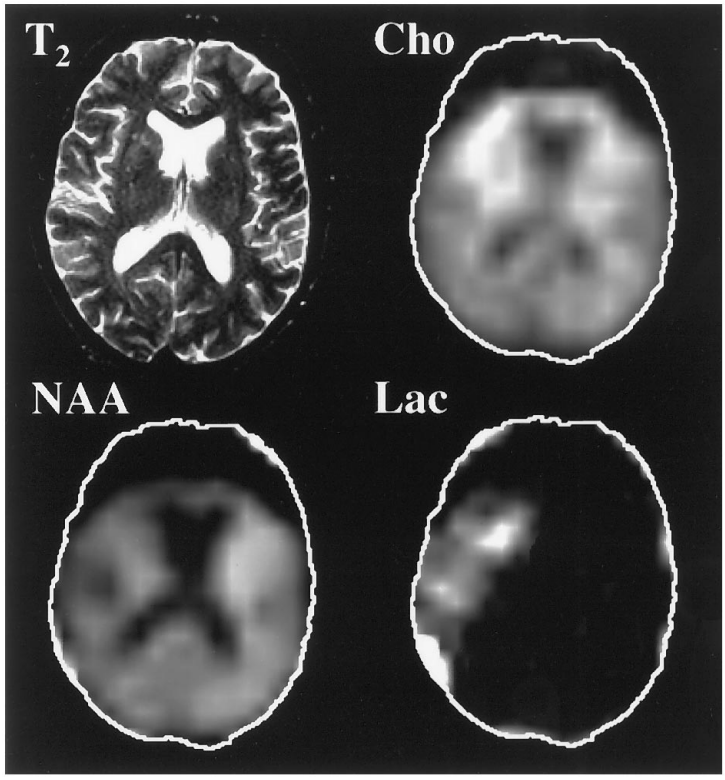

A

Fig 3. Patient 4: right internal carotid artery occlusion and low flow in right middle cerebral artery were seen at MR angiography.

A, T2-weighted MR image and MR spectrographic images of *N*-acetyl-aspartate (*NAA*), lactate (*Lac*), and choline (*Cho*) from section 2 show the presence of lactate in the right basal ganglia extending laterally and posteriorly. NAA shows a moderate decrease in a similar distribution, and choline is elevated, particularly in the anterior white matter. *Figure continues.*

left hemisphere. The patient died from massive cerebral infarction on day 3.

Patient 4 had an occlusion of the right ICA and reduced flow in the right MCA (as documented by both MR angiography and conventional X-ray angiography). Findings on T2-weighted MR images were essentially normal at the initial examination, with only slight hyperintensity in the right basal ganglia; however, significant increases in lactate were found in the right basal ganglia extending laterally to the posterior temporoparietal lobe (Figs 3A and B). NAA was only slightly decreased in a similar spatial distribution, and choline was elevated in the insular white matter. Follow-up MR studies at 7 days and at 5 months showed that the right basal ganglia had progressed to complete infarction, whereas the more lateral regions apparently resolved with no further T2 abnormalities.

Figure 4A shows T2-weighted MR images and spectroscopic images in patient 11. The T2-weighted MR images exhibited increased signal in the left temporoparietal region 8 hours after the onset of stroke. Metabolic images showed decreased NAA in the same distribution, and a slightly larger region of abnormal lactate accumulation, particularly posterior to the region of infarction (Fig 4A). Of note is the spectrum from voxel 3 of Figure 4B, which exhibits elevated lactate, near-normal levels of NAA, and no MR abnormalities, consistent with tissue potentially at risk of infarction. By day 3, this region also exhibited T2 hyperintensity (Fig 4C), suggesting that the previously ischemic tissue had progressed to infarction.

Discussion

Feasibility and Technical Considerations for Proton MR Spectroscopy in Acute Stroke

MR spectroscopic images in healthy volunteers have previously been characterized by a near-uniform distribution of NAA, with reductions only in the most caudal section and absence from the cerebrospinal fluid spaces, such as the lateral ventricles (21). With the method used in the current study, no lactate was detected in healthy subjects (Fig 1) (21), and choline was distributed, fairly uniformly, with slightly higher levels in white matter than in cortical gray matter (26). Spectroscopic im-

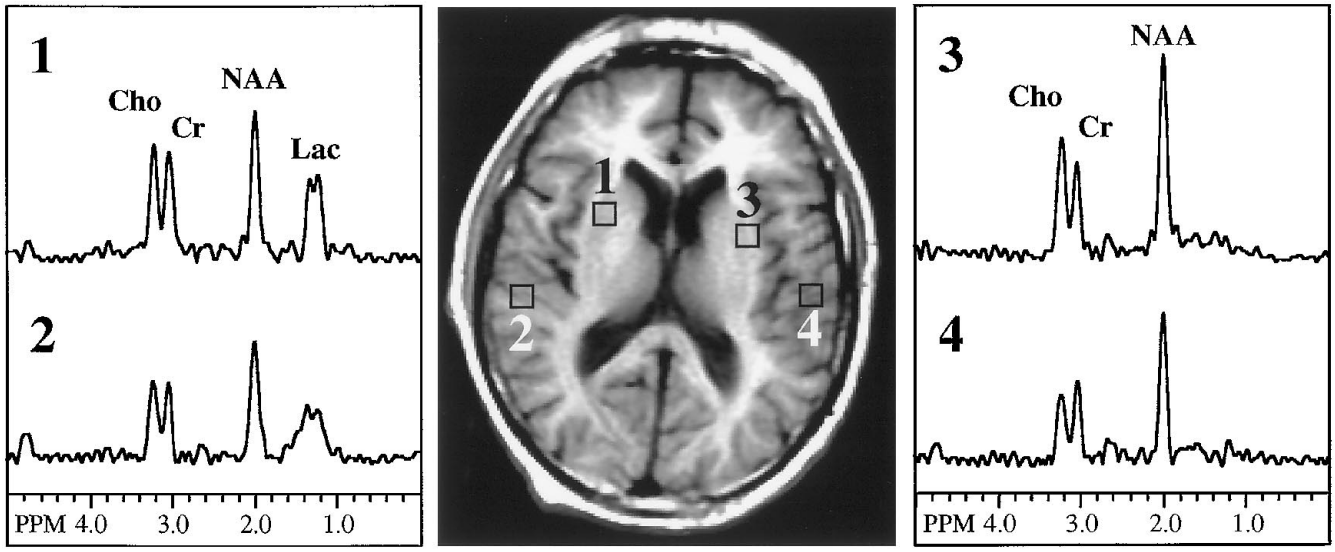

B

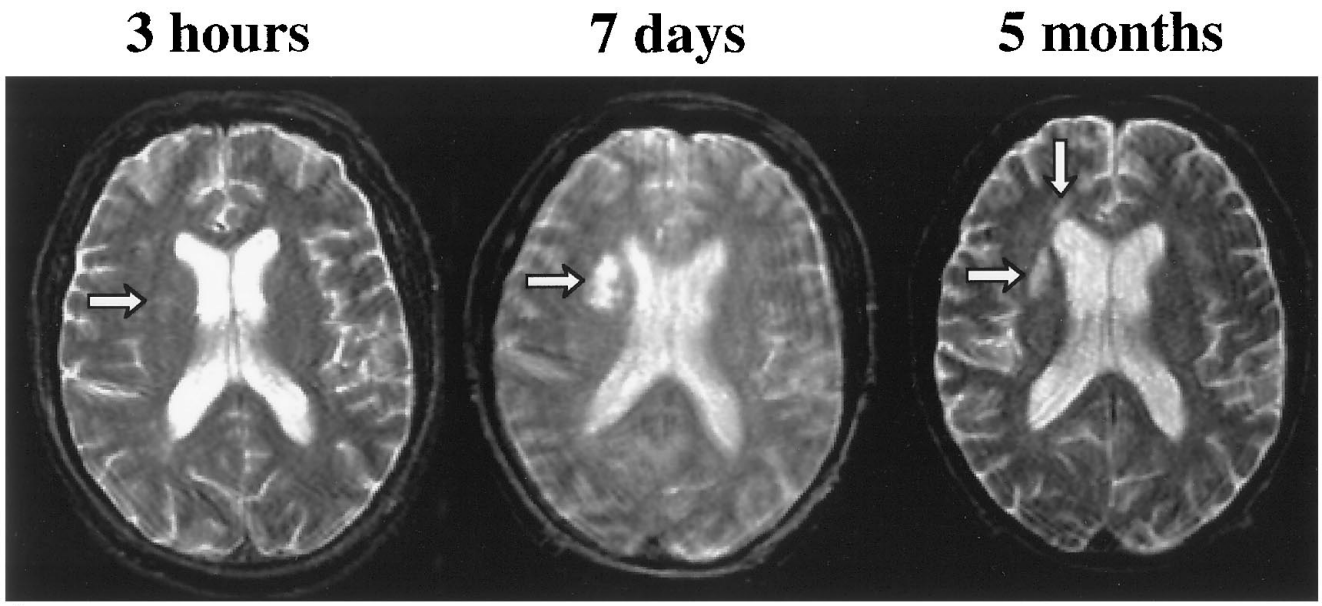

C

Fig 3, *continued.*

B, Selected proton spectra from section 2 show a relative reduction in NAA and the presence of lactate in the right anterior voxel. A voxel in a more posterolateral region of the right hemisphere again shows a small relative reduction in NAA and the presence of lactate, although smaller than anteriorly. Spectra from similar regions of interest in the left hemisphere are normal.

C, Essentially normal findings are seen on T2-weighted image at day 1, except for a slight increase in signal in the right corona radiata (*arrow*), which progresses to infarction by day 7. At 5 months, the region of hyperintensity is smaller, but a second small infarct has developed anterior to the right frontal horn of the lateral ventricle (*vertical arrow*).

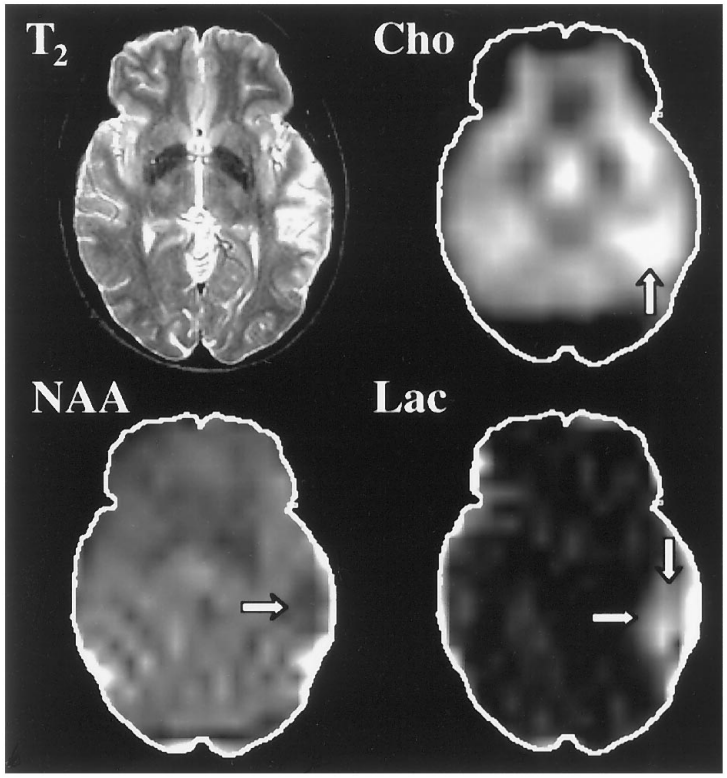

A

Fig 4. Patient 11: patent major vessels were seen at MR angiography.

A, T2-weighted MR image shows increased signal in the left temporoparietal region 8 hours after onset of stroke. MR spectroscopic images of *N*-acetyl-aspartate (*NAA*), lactate (*Lac*), and choline (*Cho*) show the presence of lactate in the left temporoparietal region and a subtle decrease in NAA (*arrows*). *Figure continues.*

ages free from lipid contamination and without significant attenuation from the effects of the outer-volume saturation pulses can be recorded to within 1 cm of the skull in most cases. However, MR spectroscopic images are susceptible to a number of artifacts; for instance, artifactual hyperintensity can sometimes result from poor water or lipid suppression, while artifactual hypointensity may result from field inhomogeneity caused by either insufficient shimming or magnetic susceptibility effects from air/tissue interfaces (particularly in the frontal regions). All of these artifacts are readily identifiable on inspection of the corresponding spectrum from the region of interest; all spectroscopic images displayed in this article are, therefore, accompanied by plots of representative spectra from appropriate regions of interest. The main uses for the spectroscopic image display mode are, therefore, as an appropriate means of screening a large number of spectra for potential abnormalities and as a visual means of evaluating the location and extent of the metabolic abnormalities. Spectral inspection, however, is always necessary to confirm the findings of the spectroscopic image display.

The quality of the MR imaging and MR spectroscopy studies of the patients was often significantly degraded as compared with that of the volunteer studies because of the effects of head motion. For the MR spectroscopy studies, patient motion resulted in reduced spectral resolution, increased lipid contamination from pericranial fat, and decreased signal-to-noise ratios; 3 (25%) of 12 patient studies were rated as poor (Table 1), and one examination was completely uninterpretable. In two studies, 1 or more sections of the 4-section sequence were uninterpretable. To reduce data acquisition time, in 2 patients, only 1 section was recorded with a reduced repetition time (1500 milliseconds instead of 2300 milliseconds for the 4-section sequence), resulting in approximately 35% reduction in data acquisition time. Future studies would be improved by use of head immobilization devices and sedation (where medically appropriate), and by the use of faster MR spectroscopy data-acquisition methods, such as multiple spin echoes (27). Nevertheless, interpretable data were obtained in 11 (91%) of 12 patients in the study, indicating feasibility even with the existing method.

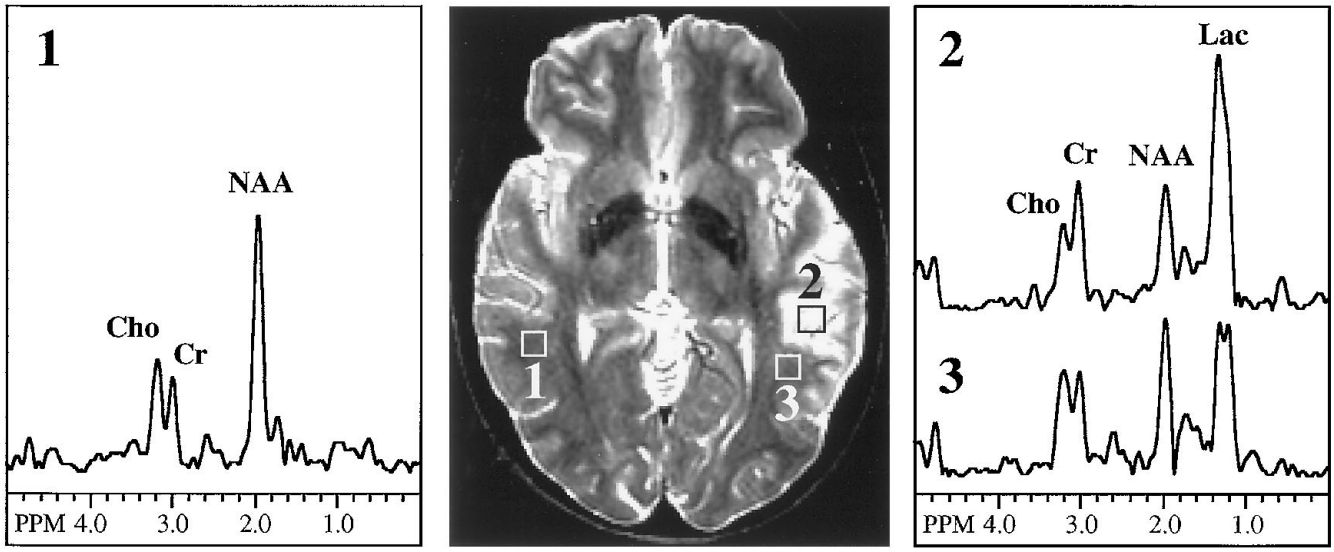

B

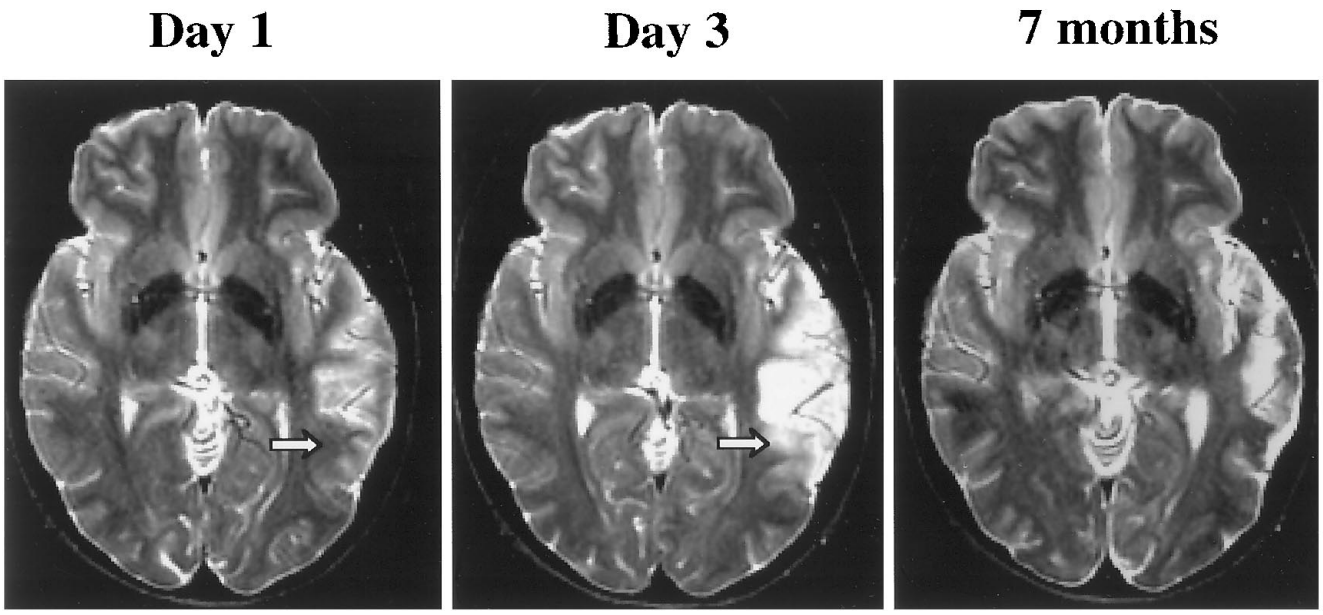

C

Fig 4, *continued.*

B, T2-weighted MR image and representative spectra from the left and right temporoparietal areas exhibit increased lactate and decreased choline on the left. Note the tissue at risk of infarction in voxel 3, which has lactate, NAA, and a normal appearance on T2-weighted MR image.

C, T2-weighted MR images 1 day, 3 days, and 7 months after onset of stroke. The region identified at risk of infarction (*arrows*) (voxel 3 on day 1 MR spectroscopic image [4B]) by day 3 shows hyperintensity on the T2-weighted MR image; however, at 7 months, the MR appearance is normal once more in this region.

Detection of Tissue at Risk of Infarction

Lactate is believed to be a sensitive indicator of ischemia in very early stroke (<24 hours); in animal studies, lactate rises rapidly from baseline levels to a steady state (proportional to the preischemic blood glucose level [28, 29]) within 10 to 15 minutes after induction of cardiac arrest (30). Lactate also increases above baseline levels in focal, incomplete ischemia once the cerebral blood flow has fallen below 20 mL/100 g per minute (31). In our study, elevated lactate was observed in all 11 patients who were scanned successfully. Lactate has also been reported to be elevated in the subacute and chronic stages of human cerebral infarction (3, 5, 7, 11, 12, 14, 16–19, 32), and also in numerous other neuropathologies. Lactate, therefore, is not necessarily a specific indicator of acute cerebral ischemia. The NAA resonance is absent or depleted from lesions known to involve neuronal/axonal loss, such as brain tumors (33), infarcts (5, 6), multiple sclerosis (34), or seizure foci (35, 36). For this reason, NAA is believed to be a neuronal/axonal marker (4). NAA reductions were observed in 10 (91%) of the 11 patients with acute stroke who were successfully studied here. Although the time course (and blood flow dependence) of the changes in NAA during cerebral ischemia have yet to be examined in detail, it has been reported that the signal from *N*-acetyl groups decreases rapidly by 10% within 1 hour after induction of global cerebral ischemia (37), and that during focal ischemia, NAA decreases more slowly, with a half-life of several hours (38). Further work, however, is required to establish the relationship between NAA levels and preservation of neuronal function and to ascertain its value as a quantitative index of neuronal loss.

Because it is generally accepted that findings on conventional spin-echo MR images are also usually normal in the first few hours after the onset of ischemia (38, 39), we propose that in patients who have sudden onset of symptoms that are consistent with cerebrovascular disease, brain regions that contain elevated lactate but that are otherwise normal in terms of their spectroscopy and imaging characteristics may represent ischemic tissue at risk of infarction. Such regions were identified in 55% of the patients in our study. However, several caveats must be considered before equating such areas with an "ischemic penumbra" (40–42). These caveats are discussed below.

Various definitions of the penumbra have been proposed (40–42), and it is apparent that different flow thresholds exist for the failure of different processes (40). For instance, protein synthesis may begin to decline and selective neuronal loss may occur at relatively high blood flows (30 to 50 mL/100 g per minute) (40), whereas functional (electroencephalographic activity) and metabolic alterations (eg, decline in pH and high energy phosphates) occur at lower blood flows (15 to 25 mL/100 g per minute) (40). The relationship between lactate, NAA levels, MR imaging parameters, and blood flow (and length of time of ischemia), and the underlying histopathologic changes have yet to be examined in detail (38). Therefore, the relationship between these imaging parameters and the conventional definitions of the ischemic penumbra remains to be established.

In a recent study of permanent, focal ischemia in a rat model, it was found that at 7 hours after MCA occlusion the area of brain that was found to contain lactate was larger than the area of histologically defined necrosis (or adenosine triphosphate depletion and acidosis) (43). One explanation for this observation is that lactate may diffuse out of the infarct into the surrounding tissue. Therefore, it has been suggested that periinfarct lactate may not be an indicator of ischemic tissue. While this cannot be discounted, other observations might negate this hypothesis. First, spectroscopic imaging studies of other lactate-containing lesions (for instance, brain tumors [44, 45]) show no evidence of perilesional lactate. Second, cerebral lactate concentrations are strictly dependent on pyruvate levels and the redox state of the cell (46); therefore, in nonischemic tissue, lactate should be converted to pyruvate and metabolized via the tricarboxylic acid cycle.

Comparison of MR spectroscopic images and MR images is complicated by the different spatial resolution of the two techniques. It is important to recognize the limited spatial resolution of the MR spectroscopic data sets and to appreciate that intervoxel signal contamination can occur between adjacent voxels (23). Therefore, a voxel of normal brain that lies immediately adjacent to a lactate-containing infarct could easily be mistaken for penumbra, since it will have a normal MR appearance but may seem to contain some lactate signal, which actually origi-

nates from the adjacent voxel. Similarly, area measurements on images obtained with the different techniques will suffer from different degrees of digitization error (ie, error will be much greater in the areas measured on the lactate images than in areas on the high-resolution MR images). Such variations in measurement error, however, do not invalidate statistical comparisons of the different area measurements.

It is well known that lipid signals can mistakenly be assigned as lactate by inexperienced spectroscopists, since they both resonate in similar regions of the proton spectrum. Contamination may occur from pericranial lipid signals when head motion occurs, and it has also been suggested that ischemic brain tissue itself may exhibit an increase in free lipid signals (47). The data acquisition method of the current study was designed to minimize lipid signals in two ways: outer-volume suppression pulses were used to saturate pericranial lipid signals, and the use of a long echo time also significantly attenuated all short T2 (lipid) resonances in the spectrum. In the data analysis, great care was taken to distinguish lactate from lipid signals. An assignment of lactate was made only if a doublet structure ($J = 7$ Hz) was observed at exactly 1.33 ppm. Normally, data sets were processed with a line-broadening of 3 Hz; in some instances, this caused the splitting of the lactate doublet to be obscured. In these cases, spectra were reprocessed without line-broadening or even slight resolution enhancement (lorentzian-to-gaussian conversion) in order to determine whether an unresolved coupling was present.

It could be argued that if the penumbra represents an area of functionally (electroencephalographically) inert yet structurally intact tissue, no neuronal loss and therefore no decline in NAA (if assumed to be a neuronal marker) would be expected. However, one of the definitions of the penumbra (41) describes selective neuronal loss as one of its features, and a recent review article also indicates that selective neuronal loss occurs at blood flows as high as 30 to 50 mL/100 g per minute (40). Therefore, in the current study, a 50% threshold for NAA levels seems reasonable for defining tissue at risk of infarction. Experiments in focal, permanent MCA occlusion in the baboon indicate a 50% loss of NAA after about 6 hours of ischemia (38); this would appear to set the lower limit for NAA levels in terms of tissue viability.

Given the above caveats, it nevertheless seems reasonable that tissue that has elevated lactate (in a clinically appropriate region that has no other spectroscopic or imaging change) is consistent with freshly ischemic brain. Identification of such regions in the early stages of stroke would represent an important criterion in selecting patients for possible therapeutic interventions. Conversely, absence of such regions, for instance, in the five patients in the current study in whom only regions containing highly depleted NAA and T2 hyperintensities were observed, would indicate that the transition to infarction has already occurred.

Although technical limitations did not allow a complete evaluation of all follow-up studies, it is nevertheless interesting to examine the fate of the tissue defined as potentially at risk at the acute stage in selected patients. For instance, in patient 4, who had an occluded right ICA and low flow in the right MCA, in the acute stage, much of the right MCA territory had elevated lactate with only small reductions in NAA (Fig 3A and B). Follow-up MR images (Fig 3C) indicated that the basal ganglia subsequently infarcted, while the more lateral region was spared; that is, one part of the penumbra infarcted while another part resolved. The sparing of the lateral, cortical region was probably due to higher blood flow in this region resulting from collateral circulation, which was not available to the basal ganglia. In contrast, the tissue at risk in patient 11 (Fig 4B, voxel 2) subsequently showed T2 MR imaging hyperintensity at 72 hours (Fig 4C), even though MR angiography consistently showed patent major vessels. Even patients with abnormal macrovascular occlusions and large infarcts had evidence of tissue at risk of infarction; for instance, patient 2, who had tandem occlusion of the left ICA and MCA (Fig 2) and high lactate, high choline, and almost complete NAA reduction in the left hemisphere, had regions closer to the midline that had lactate but also preserved NAA levels (Fig 2C, voxel 4).

Another finding of the current study, in individual cases, involved changes in the choline resonance at 3.2 ppm. In the in vivo proton spectrum, this resonance predominantly consists of glycerophosphocholine and phosphocholine (48), compounds that are precursors and breakdown products of membranes. Choline has previously been reported to be either increased (15, 16) or decreased (18) in human

cerebral infarction, as was seen in the current study (increased in five patients, decreased in six). In the patient in whom choline was observed to be elevated, the ischemic region contained a significant amount of white matter. Thus, it appears likely that the increase in choline detected here corresponded to the detection of myelin membrane breakdown products as the ischemic myelin disintegrated. Increases in choline have also been observed in other demyelinating conditions, such as multiple sclerosis (49) and adrenoleukodystrophy (50). Decreased choline (and other metabolites) probably is caused simply by reduced cellularity in the more chronic phase of infarction.

In summary, proton MR spectroscopy is feasible in the clinical setting for the evaluation of acute stroke. More studies, however, are required in both humans and in animal models of cerebral ischemia to fully evaluate the diagnostic and prognostic value of proton MR spectroscopy. Nevertheless, proton MR spectroscopy promises to play an important role in the selection and monitoring of therapeutic interventions in patients with acute stroke.

Acknowledgments

The spectroscopic imaging sequence was developed at the In Vivo NMR Center of the National Institutes of Health, Bethesda, Md, by Jeff Duyn (NIH), Joe Gillen (Pittsburgh, Pa), and Chrit Moonen (NIH). We thank Stacey Ackerman for statistical advice.

References

1. Bryan RN, Levy LM, Whitlow WD, Killian JM, Preziosi TJ, Rosario JA. Diagnosis of acute cerebral infarction: comparison of CT and MR imaging. *AJNR Am J Neuroradiol* 1991;12:611–620
2. Kertesz A, Black SE, Nicholson L, Carr T. The sensitivity and specificity of MRI in stroke. *Neurology* 1987;37:1580–1585
3. Barker PB, Gillard JH, van Zijl PCM, et al. Acute stroke: evaluation with serial proton MR spectroscopic imaging. *Radiology* 1994; 192:723–732
4. Birken DL, Oldendorf WH. *N*-acetyl-L-aspartic acid: a literature review of a compound prominent in ^{1}H-NMR spectroscopic studies of brain. *Neurosci Biobehav Rev* 1989;13:23–31
5. Berkelbach van der Sprenkel JW, Luyten PR, van Rijen PC, Tulleken CAF, den Hollander JA. Cerebral lactate detected by regional proton magnetic resonance spectroscopy in a patient with cerebral infarction. *Stroke* 1988;19:1556–1560
6. Bruhn H, Frahm J, Gyngell ML, Merboldt KD, Hanicke W, Sauter R. Cerebral metabolism in man after acute stroke: new observations using localized proton NMR spectroscopy. *Magn Reson Med* 1989;9:126–131
7. Felber SR, Aichner FT, Sauter R, Gerstenbrand F. Combined magnetic resonance imaging and proton magnetic resonance spectroscopy of patients with acute stroke. *Stroke* 1992;23:1106–1110
8. Gideon P, Henriksen O, Sperling B, et al. Early time course of *N*-acetylaspartate, creatine and phosphocreatine, and compounds containing choline in the brain after acute stroke: a proton magnetic resonance spectroscopic study. *Stroke* 1992;23:1566–1572
9. Houkin K, Kamada K, Kamiyama H, Iwasaki Y, Abe H, Kashiwaba T. Longitudinal changes in proton magnetic resonance spectroscopy in cerebral infarction. *Stroke* 1993;24:1316–1321
10. Henriksen O, Gideon P, Sperling B, Olsen TS, Jorgensen HS, Arlien SP. Cerebral lactate production and blood flow in acute stroke. *J Magn Reson Imaging* 1992;2:511–517
11. Fenstermacher MJ, Narayana PA. Serial proton magnetic resonance spectroscopy of ischemic brain injury in humans. *Invest Radiol* 1990;25:1034–1039
12. Sappey-Marinier D, Calabrese G, Hetherington HP, et al. Proton magnetic resonance spectroscopy of human brain: applications to normal white matter, chronic infarction, and MRI white matter signal hyperintensities. *Magn Reson Med* 1992;26:313–327
13. Wang Z, Bogdan AR, Zimmerman RA, Gusnard DA, Leigh JS, Ohene-Frempong K. Investigation of stroke in sickle cell disease by ^{1}H nuclear magnetic resonance spectroscopy. *Neuroradiology* 1992;35:57–65
14. Gideon P, Sperling B, Arlien-Soborg P, Olsen TS, Henriksen O. Long-term follow-up of cerebral infarction patients with proton magnetic resonance spectroscopy. *Stroke* 1994;25:967–973
15. Graham GD, Blamire AM, Rothman DL, et al. Early temporal variation in cerebral metabolites after human stroke: a proton magnetic resonance spectroscopy study. *Stroke* 1993;24:1891–1896
16. Graham GD, Blamire AM, Howseman AM, et al. Proton magnetic resonance spectroscopy of cerebral lactate and other metabolites in stroke patients. *Stroke* 1992;23:333–340
17. Petroff OA, Graham GD, Blamire AM, et al. Spectroscopic imaging of stroke in humans: histopathology correlates of spectral changes. *Neurology* 1992;42:1349–1354
18. Duijn JH, Matson GB, Maudsley AA, Hugg JW, Weiner MW. Human brain infarction: proton MR spectroscopy. *Radiology* 1992; 183:711–718
19. Hugg JW, Duijn JH, Matson GB, et al. Elevated lactate and alkalosis in chronic human brain infarction observed by 1H and 31P MR spectroscopic imaging. *J Cereb Blood Flow Metab* 1992;12: 734–744
20. Adalsteinsson E, Spielman DM, Wright GA, Pauly JM, Meyer CH, Macovski A. Incorporating lactate/lipid discrimination into a spectroscopic imaging sequence. *Magn Reson Med* 1993;30:124–130
21. Duyn JH, Gillen J, Sobering G, van Zijl PCM, Moonen CTW. Multisection proton MR spectroscopic imaging of the brain. *Radiology* 1993;188:277–282
22. Moonen CTW, van Zijl PCM. Highly efficient water suppression for in vivo proton NMR spectroscopy. *J Magn Reson* 1990;88:28–41
23. Moonen CTW, Sobering G, van Zijl PCM, Gillen J, von Kienlin M, Bizzi A. Proton spectroscopic imaging of human brain. *J Magn Reson* 1992;98:556–575
24. Marion D, Ikura M, Bax A. Improved solvent suppression in one- and two-dimensional NMR spectra by convolution of time-domain data. *J Magn Reson* 1989;84:425–430
25. Arnold DL, Matthews PM, Francis G, Antel J. Proton magnetic resonance spectroscopy of human brain in vivo in the evaluation of multiple sclerosis assessment of the load of disease. *Magn Reson Med* 1990;14:154–159

26. Soher BJ, van Zijl PCM, Duyn JH, Barker PB. Quantitative proton spectroscopic imaging of the human brain. *Magn Reson Med* 1996;35:356–363
27. Duyn JH, Moonen CTW. Fast proton spectroscopic imaging of human brain using multiple spin-echoes. *Magn Reson Med* 1993; 30:409–414
28. Rehncrona S, Rosen I, Siesjo BK. Brain lactic acidosis and ischemic cell damage, 1: biochemistry and neurophysiology. *J Cereb Blood Flow Metab* 1981;1:297–311
29. Combs DJ, Dempsey RJ, Maley M, Donaldson D, Smith C. Relationship between plasma glucose, brain lactate, and intracellular pH during cerebral ischemia in gerbils. *Stroke* 1990;21:936–942
30. Petroff OA, Prichard JW, Ogino T, Shulman RG. Proton magnetic resonance spectroscopic studies of agonal carbohydrate metabolism in rabbit brain. *Neurology* 1988;38:1569–1574
31. Crockard HA, Gadian DG, Frackowiak RS, et al. Acute cerebral ischemia: concurrent changes in cerebral blood flow, energy metabolites, pH, and lactate measured with hydrogen clearance and 31P and 1H nuclear magnetic resonance spectroscopy, II: changes during ischemia. *J Cereb Blood Flow Metab* 1987;7:394–402
32. Ford CC, Griffey RH, Matwiyoff NA, Rosenberg GA. Multivoxel 1H-MRS of stroke. *Neurology* 1992;42:1408–1412
33. Alger JR, Frank JA, Bizzi A, et al. Metabolism of human gliomas: assessment with H-1 MR spectroscopy and F-18 fluorodeoxyglucose PET. *Radiology* 1990;177:633–641
34. Matthews PM, Francis G, Antel J, Arnold DL. Proton magnetic resonance spectroscopy for metabolic characterization of plaques in multiple sclerosis. *Neurology* 1991;41:1251–1256
35. Matthews PM, Andermann F, Arnold DL. A proton magnetic resonance spectroscopy study of focal epilepsy in humans. *Neurology* 1990;40:985–989
36. Breiter SN, Arroyo S, Mathews VP, Lesser RP, Bryan RN, Barker PB. Proton MR spectroscopy in patients with seizure disorders. *AJNR Am J Neuroradiol* 1994;15:373–384
37. van Zijl PCM, Moonen CTW. In situ changes in purine nucleotide and *N*-acetyl concentrations upon inducing global ischemia in cat brain. *Magn Reson Med* 1993;29:381–385
38. Monsein LH, Mathews VP, Barker PB, et al. Irreversible regional cerebral ischemia: serial MR imaging and proton MR spectroscopy in a nonhuman primate model. *AJNR Am J Neuroradiol* 1993;14:963–970
39. Moseley ME, de Crespigny AJS, Roberts TPL, Kozniewska E, Kucharczyk J. Early detection of regional cerebral ischemia using high-speed MRI. *Stroke* 1993;24(suppl I):I-60–I-65
40. Hossman K-A. Viability thresholds and the penumbra of focal ischemia. *Ann Neurol* 1994;36:557–565
41. Hakim AM. The cerebral ischemic penumbra. *Can J Neurol Sci* 1987;14:557–559
42. Ginsberg MD, Pulsinelli WA. Ischemic penumbra, injury thresholds, and the therapeutic window for acute stroke. *Ann Neurol* 1994;36:553–554
43. Back T, Hoehn-Berlage M, Kohno K, Hossman K-A. Diffusion nuclear magnetic resonance imaging in experimental stroke: correlation with cerebral metabolites. *Stroke* 1994;25:494–500
44. Herholz K, Heindel W, Luyten P, et al. In vivo imaging of glucose consumption and lactate concentration in human gliomas. *Ann Neurol* 1992;31:319–327
45. Luyten PR, Marien AJ, Heindel W, et al. Metabolic imaging of patients with intracranial tumors: H-1 MR spectroscopic imaging and PET. *Radiology* 1990;176:791–799
46. Veech RL. The metabolism of lactate. *NMR Biomed* 1991;4:53–58
47. Saunders DE, Howe FA, van den Boogart A, McLean MA, Griffiths JR, Brown MM. Continuing ischemic damage after acute middle cerebral artery infarction in humans demonstrated by short-echo proton spectroscopy. *Stroke* 1995;26:1007–1013
48. Barker PB, Breiter SN, Soher BJ, et al. Quantitative proton spectroscopy of canine brain: in vivo and in vitro correlations. *Magn Reson Med* 1994;32:157–163
49. Davie CA, Hawkins CP, Barker GJ, et al. Detection of myelin breakdown products by proton magnetic resonance spectroscopy. *Lancet* 1993;341:630–631
50. Kruse B, Barker PB, van Zijl PCM, Duyn JH, Moonen CTW, Moser HW. Multislice proton MR spectroscopic imaging in X-linked adrenoleukodystrophy. *Ann Neurol* 1994;36:595–608